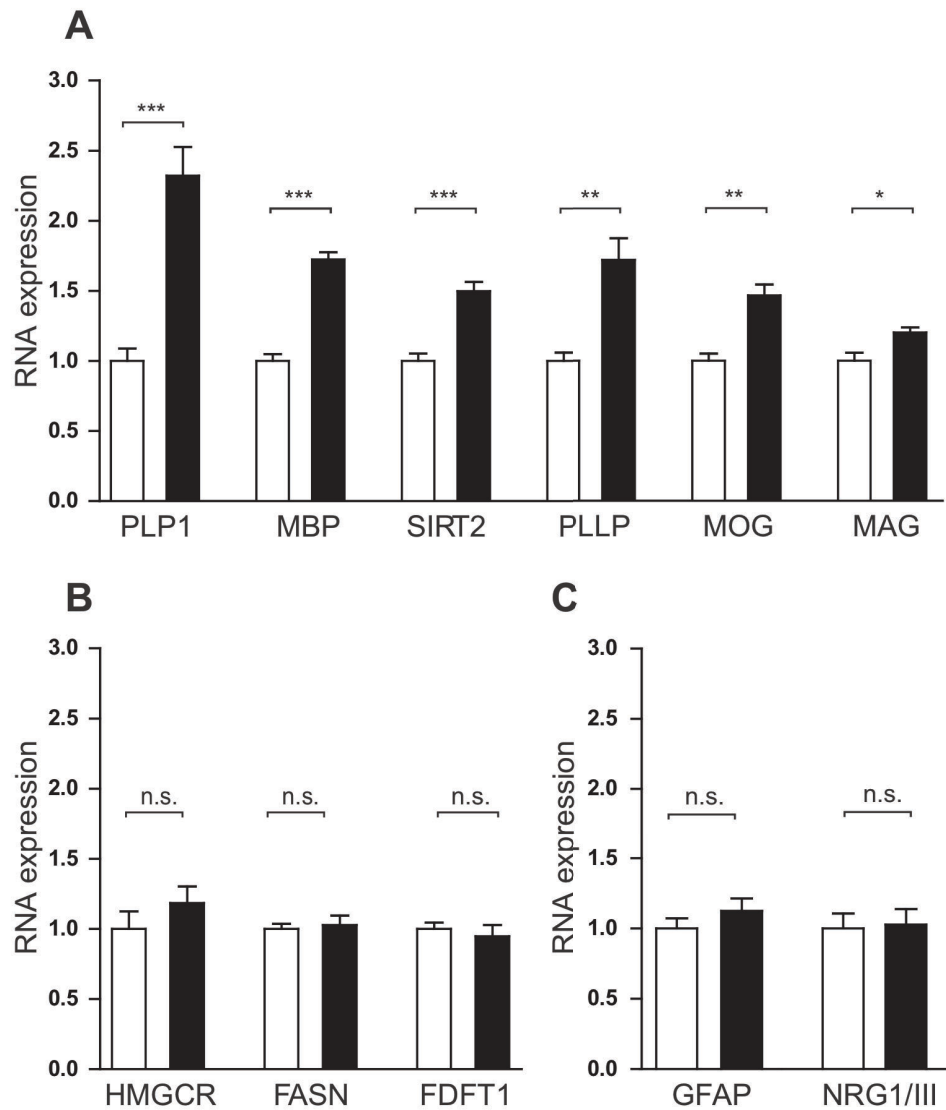


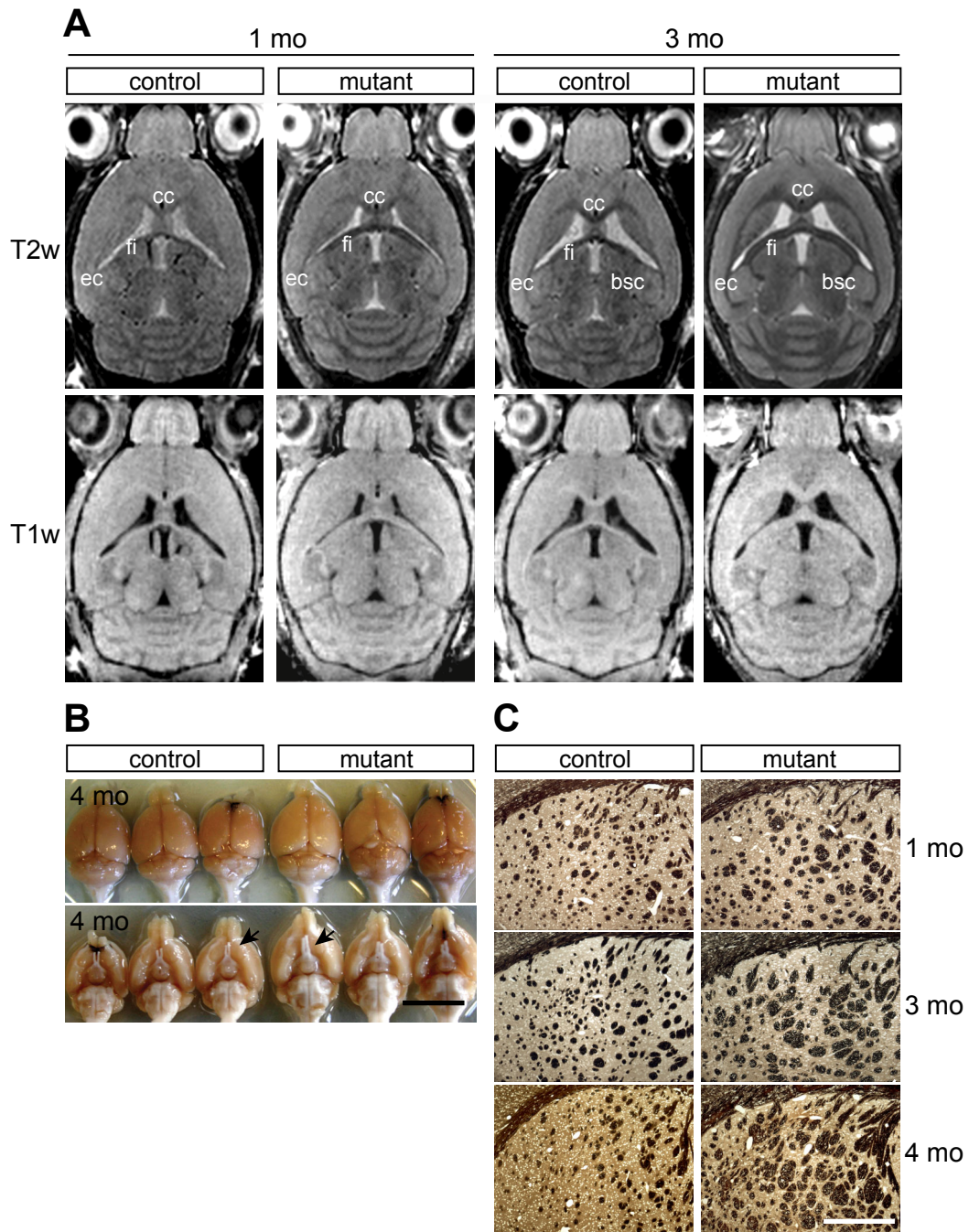
**Figure S1. Levels of PIP2 and PIP3 are dysregulated in optic nerves of *Pten* mutant mice.**

Quantification of phosphatidylinositol-4,5-bisphosphate (PIP2) and phosphatidylinositol-3,4,5-trisphosphate (PIP3) in isolated optic nerves. The analysis of lipid-associated fatty acids by gas chromatography indicates decreased levels of PIP2 and increased levels of PIP3 in mutants when compared to controls. Data are given as nmol lipid detected per pair of optic nerves (PIP2,  $p=0.0029$ ; PIP3,  $p=0.0002$ ;  $n=6$  for controls,  $n=3$  for mutants).



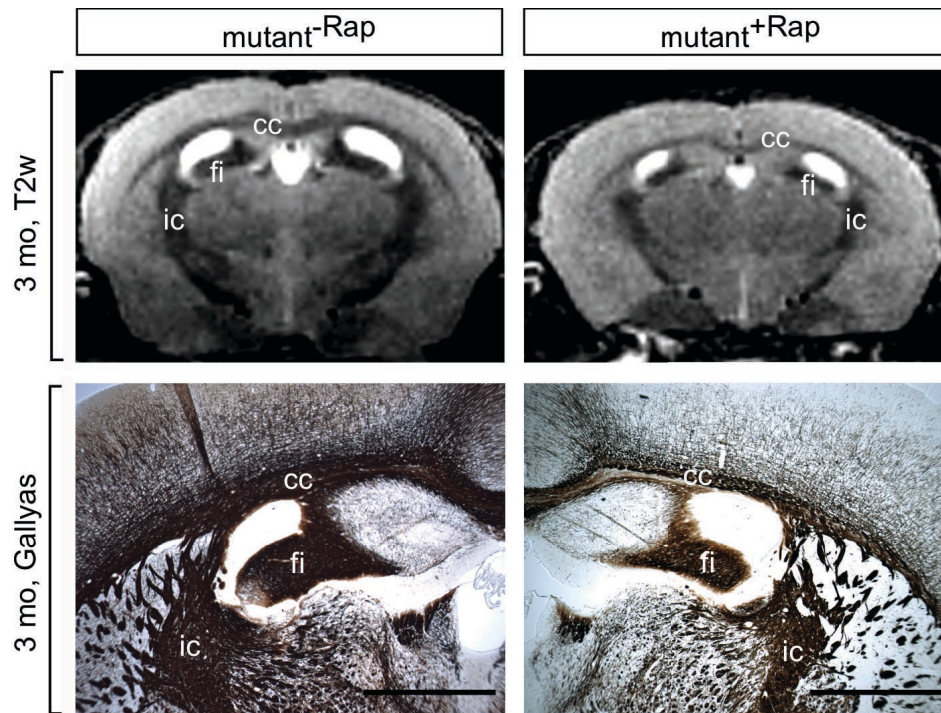
**Figure S2. Enhanced expression of myelin genes in *Pten* mutant mice.**

Quantitative RT-PCR analysis of transcripts encoding **(A)** proteins of compact and non-compact myelin (PLP1, proteolipid protein 1; MBP, myelin basic protein; SIRT2, sirtuin 2; PLLP, plasma membrane proteolipid; MOG, myelin oligodendrocyte glycoprotein; MAG, myelin-associated glycoprotein) and **(B)** enzymes of cholesterol and fatty acid-synthesis (HMGCR, 3-Hydroxy-3-Methylglutaryl-CoA reductase; FASN, fatty acid synthase; FDFT1, farnesyl diphosphate farnesyltransferase 1) from spinal cord cDNA preparations of controls (white bars) and mutants (black bars) at 1.5 months of age ( $n=5$  for each genotype). RNA expression in mutants is expressed relative to control samples that were given the arbitrary value of 1.0. In contrast to steady state transcript levels of myelin proteins, transcript levels of lipid synthesizing enzymes were not elevated in mutants when compared to controls. **(C)** For comparison, quantitative RT-PCR analysis of astroglial and neuronal transcripts (GFAP, Nrg1/III) showed no differential regulation in mutants when compared to controls. n.s., not significant ( $p>0.05$ ); \*,  $p\leq 0.05$ ; \*\*,  $p\leq 0.01$ ; \*\*\*,  $p\leq 0.001$ .



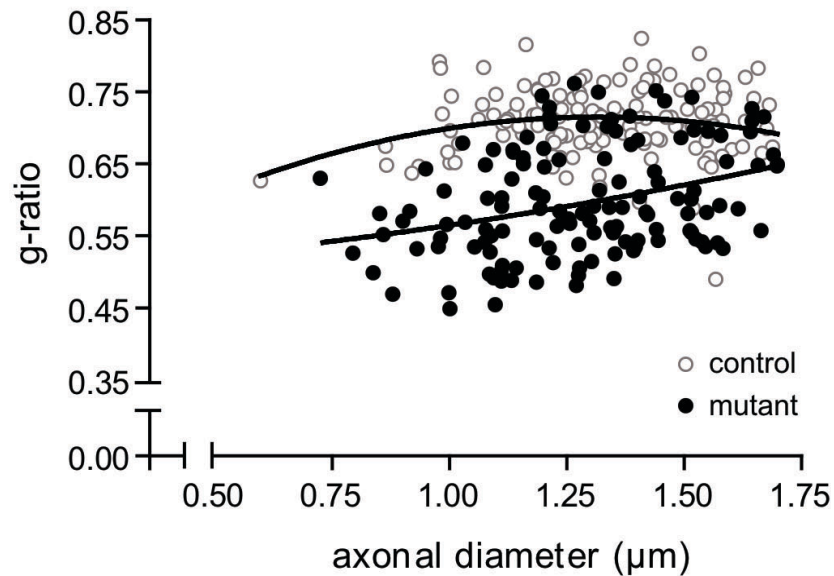
**Figure S3. Hypertrophy of CNS white matter in the absence of oligodendroglial PTEN.**

**(A)** Representative T2- and T1-weighted images (T2w, T1w) of *Pten* null mutant and control mice at the age of 1 and 3 months showing enhanced gray-white matter contrast and enlarged white matter tracts in mutants (horizontal sections). Myelinated tracts that are barely detectable in controls (e.g. brachium of superior colliculus, bsc) are clearly visible in mutants. These differences increase with age. cc, corpus callosum; ec, external capsule; fi, hippocampal fimbria. **(B)** *Pten* mutant brains and optic nerves (arrows) are enlarged compared to control littermates at 4 month of age. Scale bar, 10 mm. **(C)** Progressive enlargement of myelinated fiber bundles in the caudate putamen of mutants compared to controls when visualized by Gallyas silver impregnation at the indicated ages. Scale bar, 500  $\mu$ m.



**Figure S4. Rapamycin treatment reduces white matter hypertrophy in *Pten* mutant CNS.**

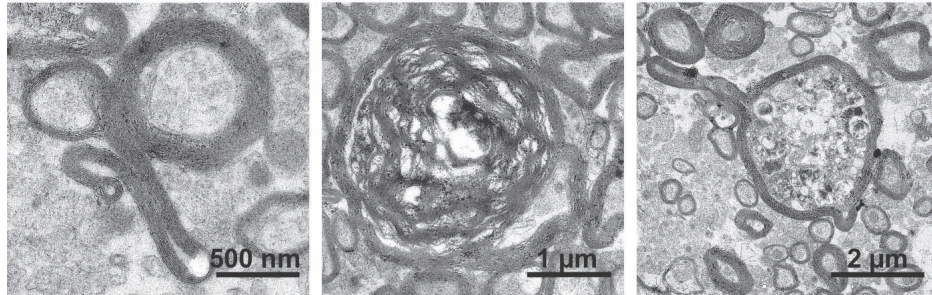
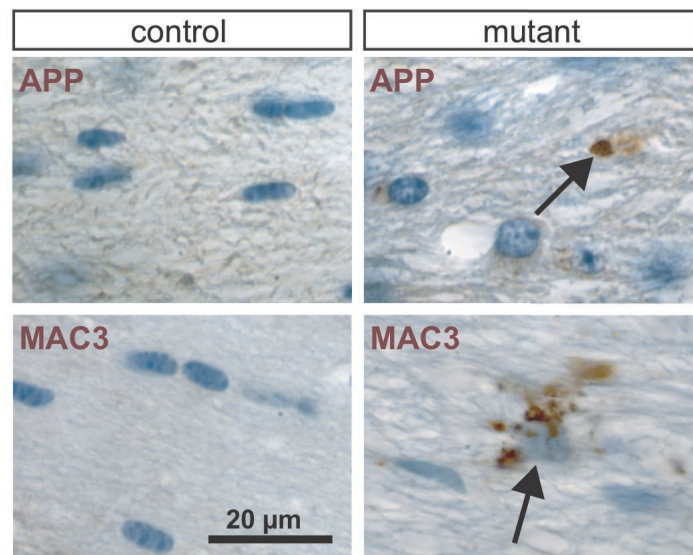
Representative images of *Pten* null mutant brains at the age of 3 months. Mice treated with vehicle (mutant<sup>-Rap</sup>) or rapamycin (mutant<sup>+Rap</sup>) from age P43 to P95 were analyzed by T2-weighted MRI (T2w) and by Gallyas silver impregnation (Gallyas). Administration of rapamycin prevented the dramatic volume increase of white matter in *Pten* ablated brains indicating a role of downstream mTOR pathway in white matter hypertrophy. cc, corpus callosum; fi, fimbria; ic, internal capsule. Scale bar, 1 mm.



**Figure S5. Small caliber axons are hypermyelinated in the sciatic nerve of *Pten* mutants (P30).**

Scatter blot for small caliber axons depicting g-ratios (ordinate) of mutant and control mice (P30;  $n=3$  per genotype) as a function of the respective axon diameter (abscissa) based on electron micrographs taken from ultrathin cross sections of sciatic nerves at comparable levels. We observed a significant decrease in g-ratios indicating hypermyelination in mutants when compared to controls. Mean g-ratios were  $0.708 \pm 0.008$  in controls and  $0.599 \pm 0.008$  in mutants ( $p=0.0007$ ;  $n=3$  per genotype).



**A****B**

**Figure S6. *Pten* mutants occasionally demonstrate myelin abnormalities and axonal pathology in the CNS.**

**(A)** Electron microscopic analysis of the corpus callosum of mutants at 3 months of age demonstrating the occasional finding of myelin abnormalities, such as evaginations of the myelin sheath (**left**) and myelin whorls (**middle**). We also noted axonal swellings as signs of axonal degeneration (**right**). **(B)** Immunostaining for amyloid precursor protein (APP) in anterior commissure and MAC3 in corpus callosum indicating axonal swellings (arrow in upper panel) and activated microglial cells (arrow in lower panel), respectively, in white matter areas of mutants when compared to controls (age 4 months).

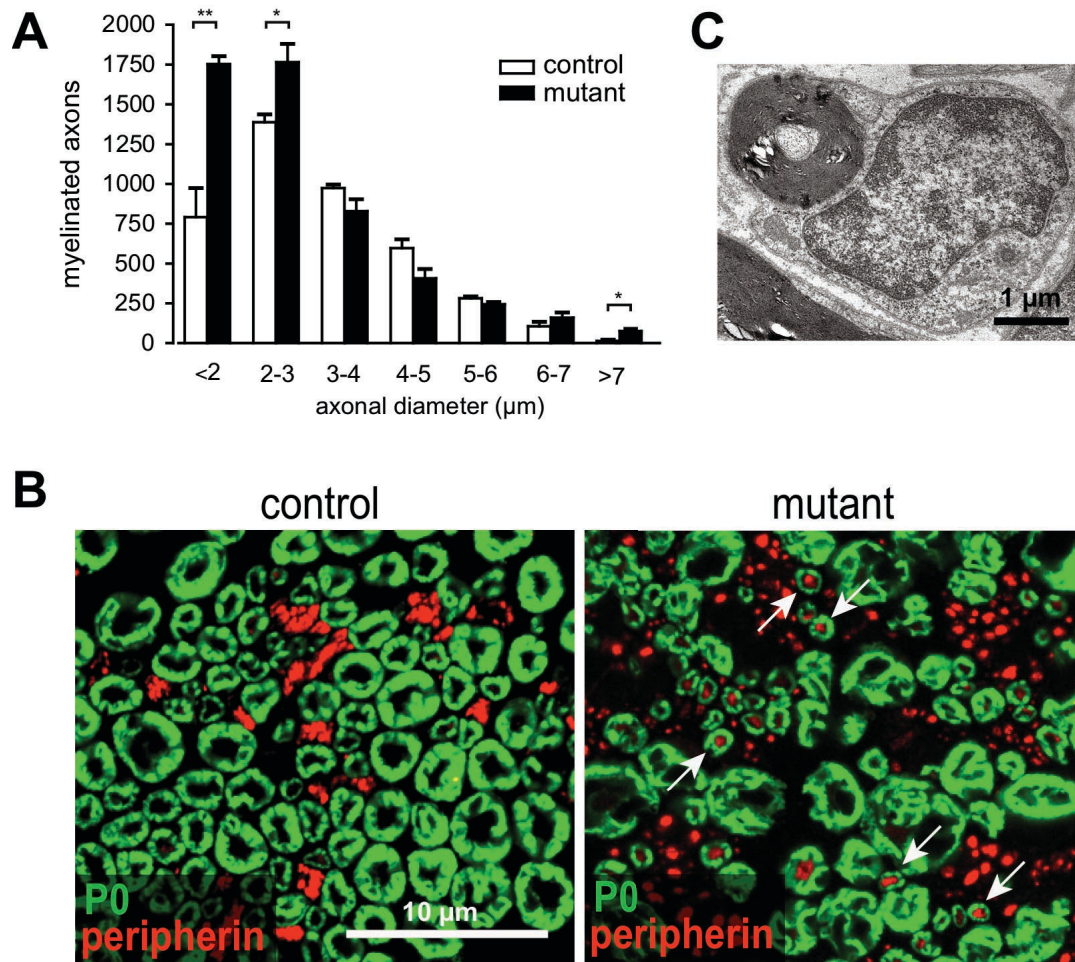


**Figure S7. *Pten* mutant Schwann cells recruit and myelinate normally non-myelinated small caliber axons.**

**(A)** Calculated number of myelinated axons per cross section (ordinate) as a function of axonal diameter (abscissa). The number of myelinated fibers in mutant nerves was significantly increased in the groups up to  $3\ \mu\text{m}$ , indicating a recruitment of small caliber axons from the pool of normally non-myelinated axons ( $<2\ \mu\text{m}$ ,  $p=0.007$ ;  $2-3\ \mu\text{m}$ ,  $p=0.04$ ;  $>7\ \mu\text{m}$ ,  $p=0.015$   $n=3$  per genotype). **(B)** Confocal analysis of sciatic nerve cross sections at the age of 1.5 months. In control mice (left), peripherin-positive C-fibers (in red) are not myelinated (P0-positive sheaths in green). In *Pten* mutant mice peripherin-positive C-fibers are often ensheathed by P0-positive membranes (arrows). **(C)** Electron micrograph of a hypermyelinated small caliber axon below  $1\ \mu\text{m}$  in diameter in a *Pten* mutant sciatic nerve that is surrounded by a thick myelin sheath.

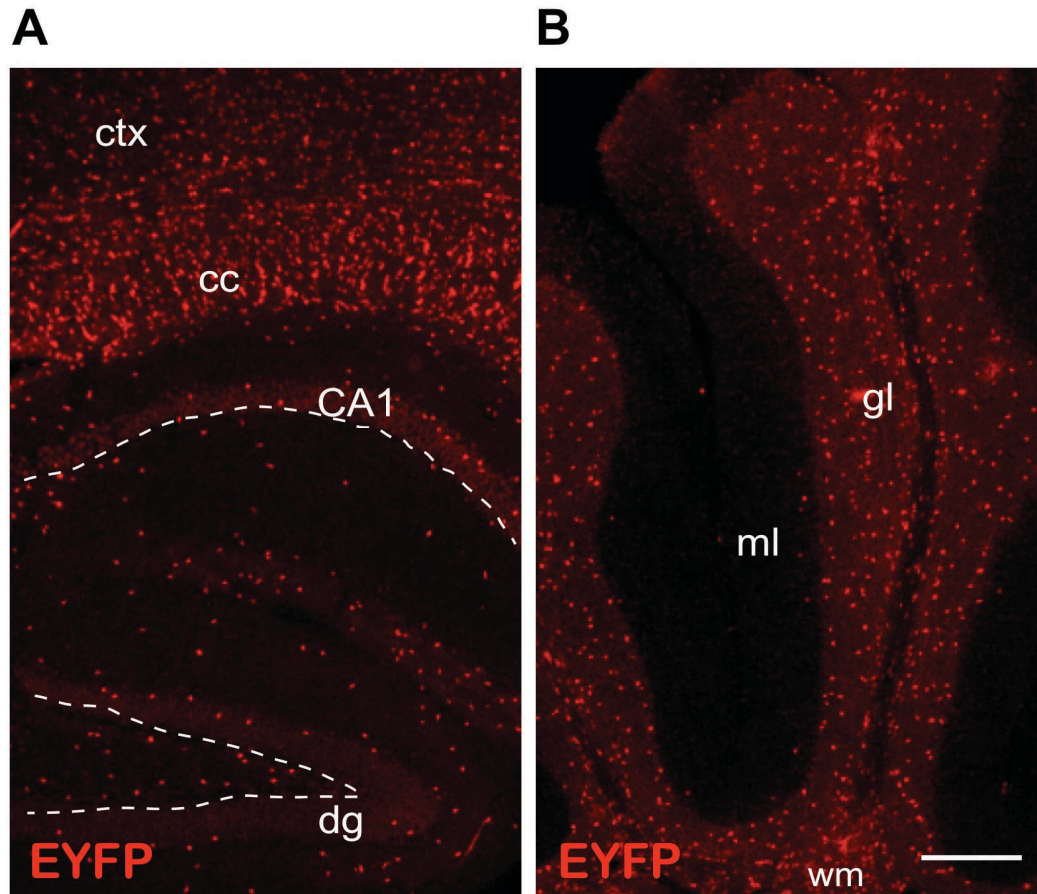


**Figure S8. Fluorescent reporter gene activation demonstrating efficient Cre-mediated recombination in adult *Plp1-CreERT2* mice.**

Sagittal forebrain (A) and cerebellar (B) sections of a double transgenic mouse harboring a *Plp1-CreERT2* transgene and a *R26R-YFP* reporter allele, analyzed 20 days after TM treatment for 10 consecutive days. The distribution of EYFP expression, detected by immunostaining (in red), suggests widespread Cre expression in myelinating oligodendrocytes. CA1, cornu ammonis area 1; cc, corpus callosum; ctx, cortex; dg, dentate gyrus; gl, granule cell layer, ml, molecular layer; wm, cerebellar white matter. Scale bar, 200  $\mu$ m.